Editors' Suggestion | Featured in Physics

Late Time Afterglow Observations Reveal a Collimated Relativistic Jet in the Ejecta of the Binary Neutron Star Merger GW170817

Davide Lazzati,[1] Rosalba Perna,[2] Brian J. Morsony,[3] Diego Lopez-Camara,[4] Matteo Cantiello,[5,6] Riccardo Ciolfi,[7,8] Bruno Giacomazzo,[8,9] and Jared C. Workman[10]

[1]*Department of Physics, Oregon State University, 301 Weniger Hall, Corvallis, Oregon 97331, USA*
[2]*Department of Physics and Astronomy, Stony Brook University, Stony Brook, New York 11794, USA*
[3]*Department of Astronomy, University of Maryland, 1113 Physical Sciences Complex, College Park, Maryland 20742-2421, USA*
[4]*CONACYT—Instituto de Astronomía, Universidad Nacional Autónoma de México, A.P. 70-264, 04510 México D.F., México*
[5]*Center for Computational Astrophysics, Flatiron Institute, 162 5th Avenue, New York, New York 10010, USA*
[6]*Department of Astrophysical Sciences, Peyton Hall, Princeton University, Princeton, New Jersey 08544, USA*
[7]*INAF, Osservatorio Astronomico di Padova, Vicolo dell'Osservatorio 5, I-35122 Padova, Italy*
[8]*INFN–TIFPA, Trento Institute for Fundamental Physics and Applications, Via Sommarive 14, I-38123 Trento, Italy*
[9]*Physics Department, University of Trento, via Sommarive 14, I-38123 Trento, Italy*
[10]*Department of Physical and Environmental Sciences, Colorado Mesa University, Grand Junction, Colorado 81501, USA*

(Received 23 March 2018; revised manuscript received 9 May 2018; published 13 June 2018)

The binary neutron star (BNS) merger GW170817 was the first astrophysical source detected in gravitational waves and multiwavelength electromagnetic radiation. The almost simultaneous observation of a pulse of gamma rays proved that BNS mergers are associated with at least some short gamma-ray bursts (GRBs). However, the gamma-ray pulse was faint, casting doubt on the association of BNS mergers with the luminous, highly relativistic outflows of canonical short GRBs. Here we show that structured jets with a relativistic, energetic core surrounded by slower and less energetic wings produce afterglow emission that brightens characteristically with time, as recently seen in the afterglow of GW170817. Initially, we only see the relatively slow material moving towards us. As time passes, larger and larger sections of the outflow become visible, increasing the luminosity of the afterglow. The late appearance and increasing brightness of the multiwavelength afterglow of GW170817 allow us to constrain the geometry of its ejecta and thus reveal the presence of an off-axis jet pointing about 30° away from Earth. Our results confirm a single origin for BNS mergers and short GRBs: GW170817 produced a structured outflow with a highly relativistic core and a canonical short GRB. We did not see the bright burst because it was beamed away from Earth. However, approximately one in 20 mergers detected in gravitational waves will be accompanied by a bright, canonical short GRB.

DOI: 10.1103/PhysRevLett.120.241103

Introduction.—The almost simultaneous detection of gravitational waves (GW170817) and of gamma rays (GRB170817A) as a result of the merger of two neutron stars in a binary [1–4] has been followed by a massive observational campaign covering a wide portion of the electromagnetic spectrum [5–11]. Early UV, optical, and IR detections were obtained within one day of the GW trigger [5,7]. Their spectra and temporal evolution were shown to be consistent with the quasithermal radiation from a kilonova [12,13], a transient powered by the radioactive decay of heavy nuclei synthesized within the merger ejecta.

In the x rays, the source was detected 9 days after the GW event by Chandra [8], while radio emission was detected a few days later [6]. X rays and radio emission were characterized by nonthermal spectra from a single power law spanning more than 8 orders of magnitude in frequency. This indicated a common origin for the high- and low-frequency emission consistent with the afterglow from a relativistic blast wave [14]. The early x-ray and radio observations were consistent with a diverse set of models for the origin of the blast wave, including a top-hat jet seen off axis [8,15–22], a mildly relativistic, isotropic fireball [23], and a structured jet [24–26].

Continued monitoring revealed that the afterglow luminosity is steadily increasing with time [9–11], a behavior that is anomalous for canonical gamma-ray bursts (GRBs) [27] and rules out simple models like the off-axis top-hat jet and the isotropic fireball [10] (see results). Any viable explanation requires the continued injection of energy in the external shock, which can be accomplished in different ways. If the central source left from the merger were still active (for example, a magnetar), its continued energy release would energize the external shock [28–30]. Alternatively, radially stratified ejecta could provide a source of energy as the slower material catches up with the external shock either with [10] or without [31] the

presence of a jet. This requires the presence of fast ejecta from the binary neutron star (BNS) merger that are significantly stratified with a very steep energy profile $E(\beta\gamma) \sim (\beta\gamma)^{-5}$, with a high-speed cutoff of at least $\beta \sim 0.5$. The mechanism that could accelerate the ejecta to such large speed is, however, not well understood.

Structured jets, on the other hand, are a natural outcome of BNS mergers, irrespectively of the detailed properties of the ambient material surrounding the merger site [10,32–35]. The propagation of a light relativistic jet through a dense environment drives a forward-reverse shock system that causes the production of a cocoon around the jet. The cocoon has high pressure but no bulk relativistic motion, shearing the jet-cocoon boundary. The ensuing structure is characterized by a narrow, highly relativistic jet, surrounded by a sheath of light but slower material and mildly relativistic wings at large angles [33]. While structured jets can be obtained with other mechanisms, this jet-cocoon mechanism is quite general and is guaranteed to produce a structured jet, fairly independent of the initial structure of the outflow and the amount of ambient material it travels through [32–35]. After it has released the prompt emission either at the photosphere [26,33] or, more likely, via shock dissipation processes [24], the structured jet propagates and drives an external shock into the interstellar medium [25,36]. Nonthermal particles and magnetic fields generated downstream the shock produce synchrotron radiation, the broadband emission that is commonly referred to as afterglow [14,37]. A structured jet seen on axis is indistinguishable from a top-hat jet; if, instead, the jet is seen off axis, differences in its structure become apparent [25,38,39].

Here, we compute multiwavelength afterglow light curves from the structured fireball expected to develop from a BNS merger [33] that also produces a canonical short GRB. We then compare the calculated light curves to the available data set for GW170817 and show that the model is in agreement with the data. With the afterglow data only, we can constrain the viewing angle to within an uncertainty of only a few degrees and we find it to be in agreement with previous constraints from independent estimates. The prompt emission from the model that we adopt is discussed in [33], where it is shown that the energetics and duration of the pulse are consistent with the observations of GW170817 [3,4]. There is tension, instead, between the predicted frequency (a few keV, in the soft x rays) and the observations (∼200 keV, in the soft gamma rays). The discrepancy is due to the assumption of a dissipationless cocoon in [33]. The observed transient, instead, calls for a shocked cocoon in which the radiation is released by the breakout of a radiation dominated shock [24,40].

Methods.—Calculation of the afterglow light curves: Light curves and spectra from the external shock were computed adopting standard techniques [37–39,41]. Our code integrates the emission over the equal arrival times surface [42] and assumes that different sections of the jet do not undergo sideways expansion [43] even after the jet comes in causal contact with its boundary (when $\Gamma < \theta_j^{-1}$). The amount of sideways expansion is a debated topic, with numerical simulations of top-hat jets suggesting a limited amount of spreading, even at late times [44]. In any case, sideways expansion has a small impact on the light curves and the assumption that we made does not affect our conclusions (see, e.g., Fig. 4 of Rossi *et al.* [39]).

The input data of our structured jet model are taken from a numerical simulation of a jet propagating through nonrelativistic ejecta from a binary neutron star merger [33]. The simulation was carried out prior to the detection of GW170817. It was initiated in three dimensions and subsequently mapped in two dimensions for the large scale evolution. Cylindrical symmetry was assumed for the afterglow calculations. The input parameters of the simulation, jet energy ($E = 10^{50}$ erg) and opening angle ($\theta_j = 16°$), yielding $E_{\rm iso} = 2.6 \times 10^{51}$, were chosen to mimic as best as possible a typical short GRB [45]. The jet leaving the ambient material of the merger has been hydrodynamically collimated into a narrower $\text{theta}_j = 5°$ cone, with an isotropic equivalent energy $E_{\rm iso} = 10^{52}$ erg. Previous studies [46–49] had confirmed that the jet can survive the interaction, at least in some cases, and in this work we concentrate on the polar structure of the ejecta at large radii.

As typical for afterglow calculations, our models depend on the microphysical shock parameters that describe the particle distribution and magnetic field intensity downstream the shock. A fraction ϵ_e of the shock energy is given to electrons, and all the electrons are accelerated in a power-law distribution $n(\gamma) \propto \gamma^{-p_{\rm el}}$. In addition, a fraction ϵ_B of the shock energy is assumed to be converted into a tangled magnetic field. Given the location of GW170817 in the outskirts of an early type galaxy [5,7], we compute our models for a uniform interstellar medium of number density $n_{\rm ISM}$. The last free parameter is the orientation of the line of sight with respect to the jet axis. Neither the blast wave energy nor its initial Lorentz factor is a free parameter in our model. They are both determined uniquely by the polar angle. Figure 1 shows the resulting radio (8 GHz) and x-ray (1 keV) light curves for different viewing angles. The same code was used also for the calculation of afterglow light curves from top-hat jets and isotropic fireballs. A top-hat model is a jet with constant energy and Lorentz factor within a specified jet angle θ_j. The jet has sharp edges, and the energy and velocity outside of the jet angle are set to 0.

In the case of isotropic fireballs, the model has six free parameters (one more than for structured jets) since the blast wave energy E and the initial Lorentz factor Γ_0 are free, but the observer angle is irrelevant. In the case of a top-hat jet, the model has seven free parameters. In addition to the five of the structured jet, one has to consider the jet's isotropic equivalent energy $E_{\rm iso}$ and the jet opening angle θ_j. Since we are concerned with top-hat jets seen off axis,

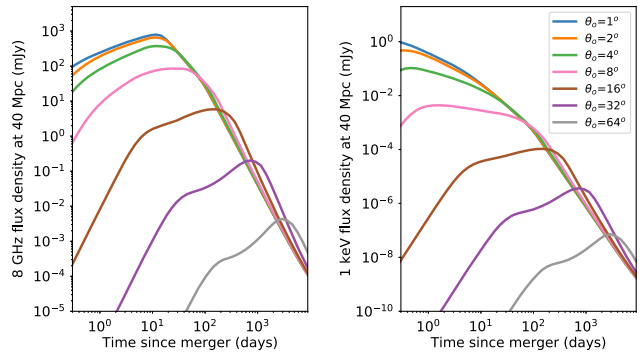

FIG. 1. Light curves of the afterglow of a structured jet calculated at a frequency of 8 GHz (left panel) and 1 keV (right panel) for several observers. Viewing angles are indicated in the legend. The parameters used for these models are $\epsilon_e = 10^{-2}$, $\epsilon_B = 10^{-3}$, $p_{\rm el} = 2.3$, and $n_{\rm ISM} = 10^{-4}$ cm^{-3}.

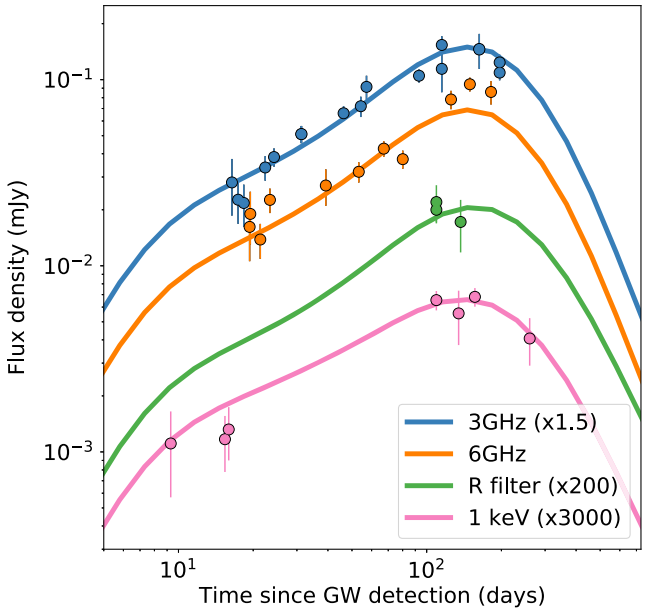

FIG. 2. The radio, optical, and x-ray light curves from a structured jet model are shown in blue (3 GHz), yellow (6 GHz), green (R band), and pink (x rays), respectively. For viewing purposes, all but the 6 GHz curves have been multiplied by a constant (as specified in the legend). Radio and x-ray measurements with uncertainties are shown with filled symbols. Additional data at other radio frequencies have been used in the fit but are not shown because they are sparse and would overcrowd the figure. The optical light curve at early time was dominated by the kilonova emission, which is not considered in our modeling. The model shown has $\chi^2 = 69$ with 56 degrees of freedom. The observer lies at an angle of 33° from the jet axis and the fireball propagates in a uniform external medium with number density $n_{\rm ISM} = 4.2 \times 10^{-3}$ cm^{-3}. The figure includes the most recent Chandra observation ([59], the x-ray datum at 260 days), which is not fit but just overlaid on the best-fit curves from the data at pervious times.

the initial Lorentz factor is irrelevant, and we set it to $\Gamma_0 = 300$ for all top-hat models. While more sophisticated models for top-hat jets are available [50], in order to be able to directly compare the isotropic, structured, and top-hat jets it is fundamental to adopt the same code in the calculation of the three.

Data modeling.—Several previous publications have considered structured jets as a plausible explanation for the data of GW170817 [21,51–54], while only one publication presents a formal fit to the data analogous to what we present here [55]; however, their structured model is analytical and not self-consistently derived from simulations of jet propagation. Our fitting data set is the result of a complete collection (to our best knowledge) of data published in the literature [6,8–11,15,16,19,56–58]. Since the calculation of top-hat and structured jet models is numerically intensive, we have performed a Markov chain Monte Carlo analysis. We have constructed a grid of models for all three cases for a set of parameter values. We then draw a random selection of the parameter set and perform a multilinear interpolation of the model grid in log space to derive the model at the desired value of the parameters. We then compute the χ^2 of said model with respect to the data. The parameter set is defined to be behavioral if the probability value is more than 0.0027, corresponding to 3σ. Figure 2 shows the best-fit model for the structured jet from Table I compared to data in four selected bands: 3 GHz, 6 GHz, optical, and 1 keV. Figure 3 shows all the behavioral models in the same bands in four panels. Models are color-coded according to their probability. The corner plot of parameter degeneracy is shown in Fig. 4. It shows that there is a pronounced degeneracy between the interstellar density and the viewing angle. Finally, in Fig. 5 we compare the best fits of the three models with one another.

Results.—We have computed the afterglow light curve (see methods and Figs. 1 and 3) from a structured jet obtained from a numerical simulation of relativistic outflows from BNS mergers [33]. A frame of the simulation is shown in the left panel of Fig. 6 and the energy and Lorentz factor profiles are shown in the lower right panel of the same figure. The structured jet from our simulation does not have a well-identified core, unlike a top-hat jet. As seen in the lower panel of Fig. 6, the core of the jet extends out to an off-axis angle of approximately 5°, which carries $\sim 10^{52}$ erg of isotropic equivalent energy. These properties are on the high side of short GRB population studies, yet consistent with a short GRB observed on axis [60], especially considering that only a fraction of the kinetic energy is converted to radiant energy. The core Lorentz factor of order 100 is also consistent with constraints from the prompt emission of on-axis events [61]. With the exception of the on-axis models with $\theta_o < 10°$, all our synthetic light curves are characterized by a fast early phase (proportional to t^3), a break at a few days followed by a slow luminosity increase, a maximum at a few months to

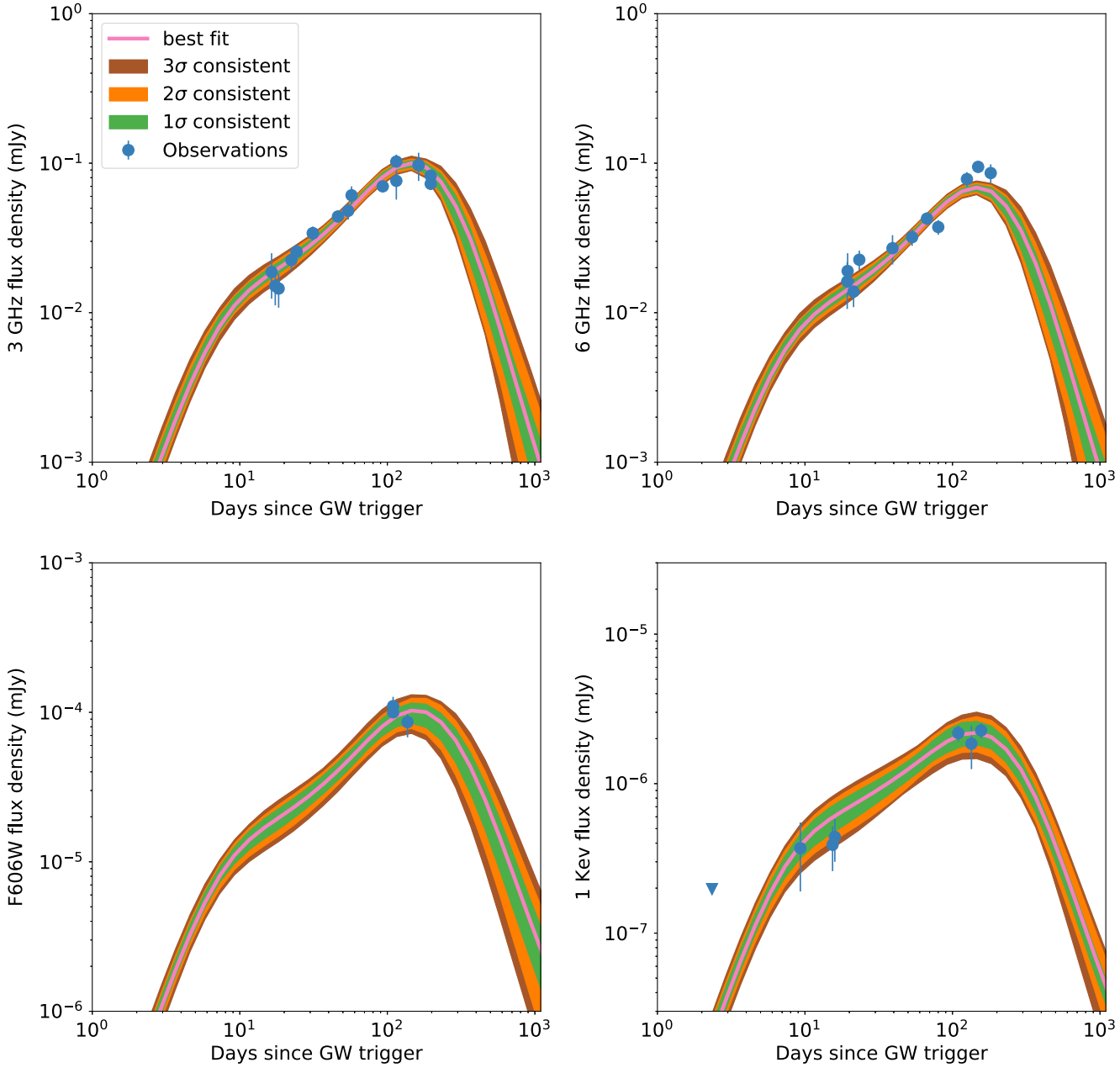

FIG. 3. Light curves and their uncertainty areas compared with the measurement of the afterglow of GW170817. The pink line is the best-fit model. The green shaded area is the envelope of all models consistent with the data at the 1σ level, orange is consistent at the 2σ level, and brown is consistent at the 3σ level. Data are displayed with solid blue markers. All models were fit simultaneously to the entire multiwavelength data set. The upper left panel shows the 3 GHz light curve, the upper right panel shows the 6 GHz light curve, the bottom left panel shows the 606 nm light curve, and the bottom right panel shows the 1 keV light curve.

years after the merger, and a final decay over several years (see Fig. 1). The material that travels directly along the line of sight is responsible for the early emission [10]. The first break at a few days is due to the deceleration of that material once it accumulates enough interstellar mass. As time progresses, material that travels at increasingly large angles with respect to the line of sight decelerates and its radiation becomes visible. To the observer, it appears that the fireball's energy has increased and therefore the afterglow brightens. Eventually, the jet core that carries most of the energy comes into view. This corresponds to the maximum in the light curves and happens between a few months and a few years after the merger, depending on a combination of the jet's energy and Lorentz factor and of the interstellar density. Figure 6 shows a decomposition of the 3 GHz light curve in five components. Most of the radiation comes from the region of the outflow between the line of sight and the core (regions A–C in the figure), with

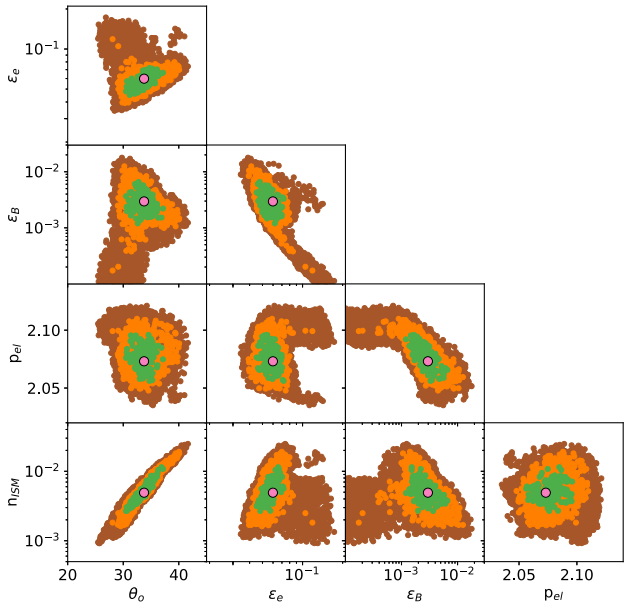

FIG. 4. Corner plot showing the degeneracy of the fit parameters for the structured jet model. A strong degeneracy is evident between the interstellar density and the observing angle. The meaning of different colors is the same as in Fig. 3.

the outer regions (D and E) contributing a negligible amount of flux.

The radio, optical, and x-ray light curves from the best-fit model are shown in Fig. 1 and the spectra at two epochs are

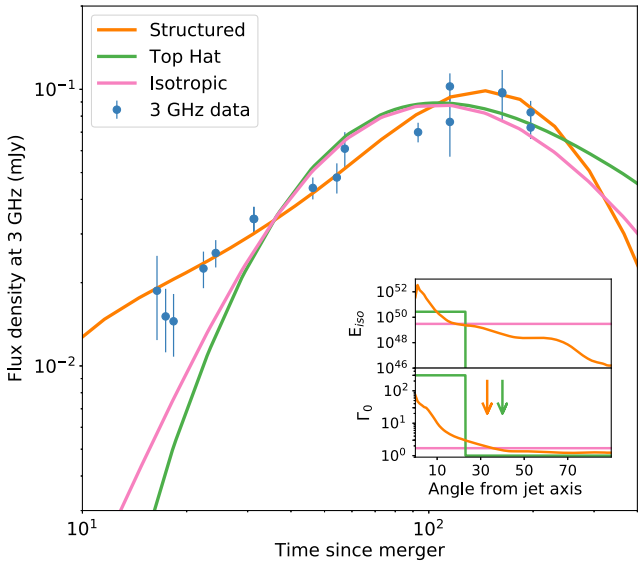

FIG. 5. Comparison among the best fits 3 GHz light curves for the three model structures discussed: an isotropic fireball (pink), an off-axis, top-hat jet (green), and a structured jet (orange). Data at 3 GHz are shown with solid blue symbols, but the fits were performed on all of the multiwavelength data set. The inset shows the best-fit energy and Lorentz factor profiles of the three models. The vertical arrows show the location of the observer in the top-hat and structured models.

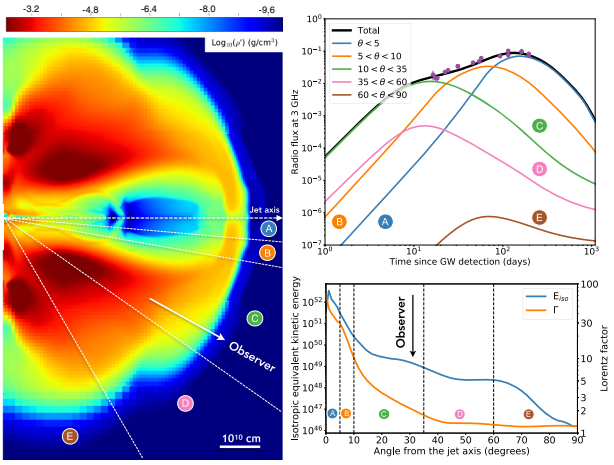

FIG. 6. Left panel: pseudocolor density image of the hydrodynamic numerical simulation of a short gamma-ray burst jet from a binary neutron star merger used to compute the afterglow light curves [33]. The propagation of the jet through nonrelativistic ejecta in the vicinity of the merger site causes the emergence of a structured jet, with a light, fast core (the low-density, blue region) and less energetic, slower wings (the orange and green material surrounding the jet). The line of sight to the observer (lying at 33° from the jet axis) is shown with a white arrow. The polar distribution of energy and velocity of the ejecta is shown in the bottom right panel. The top right panel shows the best-fit afterglow model decomposed into radiation coming from the core of the jet (blue), the fast wings of the jet (orange), the material moving along the line of sight (green), and material at large angles (pink and brown, which do not contribute to the observed afterglow emission). The solid black line is the sum of the colored lines.

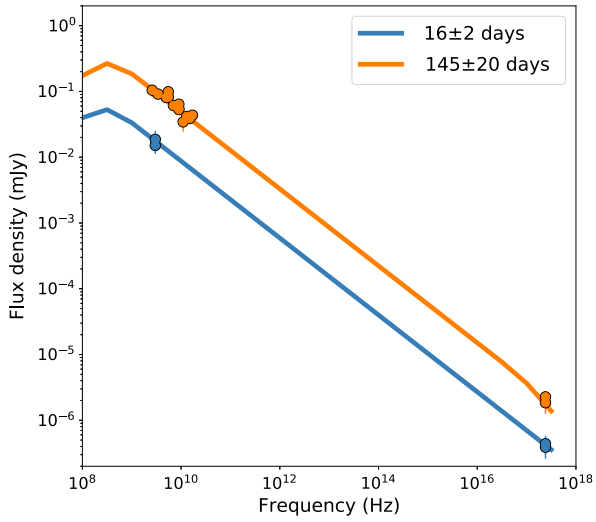

FIG. 7. Broadband spectra of the transient produced by the external shock from a structured jet seen off axis. The afterglow spectrum from the radio to the x rays is shown at two epochs. In blue is the time of the earliest radio and x-ray measurements (∼16 days after the trigger); in orange is the epoch at which the radio light curve peaks, approximately 145 days after the trigger. The displayed data have been taken within a few days of the time at which the spectra were computed (as specified in the legend).

TABLE I. Parameters and statistical properties of the best fit for the three models analyzed.

	Isotropic	Top hat	Structured
χ^2/d.o.f.	286/55	266/54	69/56
Probability	$< 10^{-10}$	$< 10^{-10}$	0.11 (1.6σ)
$E_{\rm iso}$ (erg)	2.5×10^{49}	5.7×10^{51}	...
Γ_0	1.8	...	...
θ_j (degrees)	...	23	...
θ_o (degrees)	...	39	$33^{+4}_{-2.5}$
ϵ_e	0.03	0.01	0.06 ± 0.01
ϵ_B	0.0002	0.003	0.0033 ± 0.002
$p_{\rm el}$	2.065	2.07	2.07 ± 0.01
$n_{\rm ISM}$ (cm^{-3})	6.8×10^{-4}	9.1×10^{-4}	$(4.2^{+8.5}_{-1.6}) \times 10^{-3}$

shown in Fig. 7. Data are shown for comparison on both figures. The best-fit model has a statistically acceptable χ^2 (69 for 56 degrees of freedom, with probability $p = 11\%$) and it is characterized by a viewing angle $\theta_o = 33^{+4}_{-2.5}$ in degrees, consistent with other constraints on the viewing geometry.

In addition, we have also attempted to fit a low-Γ isotropic fireball (without any radial stratification) and a top-hat jet model to the data. We find that these two models can be rejected at very high statistical confidence. The comparison of the best fit of the three models is shown in Fig. 5, and the details of the fits are reported in Table I.

Conclusions.—The goodness of our fit and the consistency of our results with other independent measurements strongly suggest that binary neutron star mergers do produce short GRBs, as predicted many years ago [62] and supported by several lines of circumstantial evidence from their host galaxies, locations, and rate [63]. We found that within the structured jet-cocoon model, all observations can be reconciled if the observer lies at a viewing angle $\theta_o \approx 30°$. Such viewing geometry is consistent with the GW amplitude [1] ($\theta_o \lesssim 30°$), with the prompt gamma-ray energetics and duration [33] ($20° \lesssim \theta_o \lesssim 40°$), the kilonova characteristics [64] ($15° \lesssim \theta_o \lesssim 35°$), and the afterglow modeling presented here.

Future observations could lend further support to this conclusion. First, due to its relative proximity to Earth and radio brightness, the remnant of GW170817 can be resolved with the very large baseline interferometer [65,66]. We expect that at the time of maximum afterglow luminosity the physical size of the remnant will be approximately one parsec, or 4.6 milli arcsec, compared to the very large baseline interferometer angular resolution of 0.3 milli arcsec at 30 GHz. Asymmetry in the ejecta brightness should be prominent before and around the peak time in the structured jet scenario, while the remnant would be fairly spherical in the radially stratified case. Linear polarization with consistent position angle peaking around the maximum brightness of the afterglow would also confirm the presence of a jet [39,65]. Finally, direct confirmation of the association is possible. Once every 20 events, we expect the line of sight to be within the jet cone and a bright, on-axis short GRB to be observed in coincidence with a GW signal from the merger.

We thank J. Ivan Castorena for help with gathering observational data from the literature. D. L. acknowledges support from NASA ATP Grant No. NNX17AK42G. R. P. acknowledges support by NSF Grant No. AST-1616157. The Flatiron Institute is supported by the Simons Foundation. B. J. M. is AAAS Science and Technology Policy Fellow.

[1] B. P. Abbott, R. Abbott, T. D. Abbott, F. Acernese, K. Ackley, C. Adams, T. Adams, P. Addesso, R. X. Adhikari, V. B. Adya *et al.*, Phys. Rev. Lett. **119**, 161101 (2017).
[2] B. P. Abbott, R. Abbott, T. D. Abbott, F. Acernese, K. Ackley, C. Adams, T. Adams, P. Addesso, R. X. Adhikari, V. B. Adya *et al.*, Astrophys. J. **848**, L12 (2017).
[3] A. Goldstein *et al.*, Astrophys. J. **848**, L14 (2017).
[4] V. Savchenko *et al.*, Astrophys. J. **848**, L15 (2017).
[5] D. A. Coulter, R. J. Foley, C. D. Kilpatrick, M. R. Drout, A. L. Piro, B. J. Shappee, M. R. Siebert, J. D. Simon, N. Ulloa, D. Kasen, B. F. Madore, A. Murguia-Berthier, Y.-C. Pan, J. X. Prochaska, E. Ramirez-Ruiz, A. Rest, and C. Rojas-Bravo, Science **358**, 1556 (2017).
[6] G. Hallinan *et al.*, Science **358**, 1579 (2017).
[7] M. Soares-Santos *et al.* (Dark Energy Survey, and Dark Energy Camera GW-EM Collaboration), Astrophys. J. **848**, L16 (2017).
[8] E. Troja *et al.*, Nature (London) **551**, 71 (2017).
[9] R. Margutti, K. D. Alexander, X. Xie, L. Sironi, B. D. Metzger, A. Kathirgamaraju, W. Fong, P. K. Blanchard, E. Berger, A. MacFadyen, D. Giannios, C. Guidorzi, A. Hajela, R. Chornock, P. S. Cowperthwaite, T. Eftekhari, M. Nicholl, V. A. Villar, P. K. G. Williams, and J. Zrake, Astrophys. J. **856**, L18 (2018).
[10] K. P. Mooley *et al.*, Nature (London) **554**, 207 (2018).
[11] J. J. Ruan, M. Nynka, D. Haggard, V. Kalogera, and P. Evans, Astrophys. J. **853**, L4 (2018).
[12] D. Kasen, B. Metzger, J. Barnes, E. Quataert, and E. Ramirez-Ruiz, Nature (London) **551**, 80 (2017).
[13] E. Pian *et al.*, Nature (London) **551**, 67 (2017).
[14] P. Mészáros and M. J. Rees, Astrophys. J. **476**, 232 (1997).
[15] K. D. Alexander *et al.*, Astrophys. J. **848**, L21 (2017).
[16] D. Haggard, M. Nynka, J. J. Ruan, V. Kalogera, S. B. Cenko, P. Evans, and J. A. Kennea, Astrophys. J. **848**, L25 (2017).
[17] K. Ioka and T. Nakamura, Prog. Theor. Exp. Phys. **2018**, 043E02 (2018).
[18] S. Kim *et al.*, Astrophys. J. **850**, L21 (2017).
[19] R. Margutti, E. Berger, W. Fong, C. Guidorzi, K. D. Alexander, B. D. Metzger, P. K. Blanchard, P. S. Cowperthwaite, R. Chornock, T. Eftekhari, M. Nicholl, V. A. Villar, P. K. G. Williams, J. Annis, D. A. Brown, H. Chen, Z. Doctor, J. A. Frieman, D. E. Holz, M. Sako, and M. Soares-Santos, Astrophys. J. **848**, L20 (2017).

[20] A. Murguia-Berthier, E. Ramirez-Ruiz, C. D. Kilpatrick, R. J. Foley, D. Kasen, W. H. Lee, A. L. Piro, D. A. Coulter, M. R. Drout, B. F. Madore, B. J. Shappee, Y.-C. Pan, J. X. Prochaska, A. Rest, C. Rojas-Bravo, M. R. Siebert, and J. D. Simon, Astrophys. J. **848**, L34 (2017).

[21] D. Xiao, L.-D. Liu, Z.-G. Dai, and X.-F. Wu, Astrophys. J. **850**, L41 (2017).

[22] X.-B. He, P.-H. T. Tam, and R.-F. Shen, Res. Astron. Astrophys. **18**, 043 (2018).

[23] O. S. Salafia, G. Ghisellini, G. Ghirlanda, and M. Colpi, arXiv:1711.03112 [Astron. Astrophys. (to be published)].

[24] M. M. Kasliwal *et al.*, Science **358**, 1559 (2017).

[25] G. P. Lamb and S. Kobayashi, Mon. Not. R. Astron. Soc. **472**, 4953 (2017).

[26] D. Lazzati, A. Deich, B. J. Morsony, and J. C. Workman, Mon. Not. R. Astron. Soc. **471**, 1652 (2017).

[27] J. A. Nousek *et al.*, Astrophys. J. **642**, 389 (2006).

[28] S. Ai, H. Gao, Z.-G. Dai, X.-F. Wu, A. Li, and B. Zhang, arXiv:1802.00571.

[29] J.-J. Geng, Z.-G. Dai, Y.-F. Huang, X.-F. Wu, L.-B. Li, B. Li, and Y.-Z. Meng, Astrophys. J. **856**, L33 (2018).

[30] B. Li, L.-B. Li, Y.-F. Huang, J.-J. Geng, Y.-B. Yu, and L.-M. Song, arXiv:1802.10397 [Astrophys. J. Lett. (to be published)].

[31] K. Hotokezaka, K. Kiuchi, M. Shibata, E. Nakar, and T. Piran, arXiv:1803.00599.

[32] M. A. Aloy, H.-T. Janka, and E. Müller, Astron. Astrophys. **436**, 273 (2005).

[33] D. Lazzati, D. López-Cámara, M. Cantiello, B. J. Morsony, R. Perna, and J. C. Workman, Astrophys. J. **848**, L6 (2017).

[34] O. Gottlieb, E. Nakar, and T. Piran, Mon. Not. R. Astron. Soc. **473**, 576 (2018).

[35] A. Kathirgamaraju, R. B. Duran, and D. Giannios, Mon. Not. R. Astron. Soc. **473**, L121 (2018).

[36] Z.-P. Jin, X. Li, H. Wang, Y.-Z. Wang, H.-N. He, Q. Yuan, F.-W. Zhang, Y.-C. Zou, Y.-Z. Fan, and D.-M. Wei, Astrophys. J. **857**, 128 (2018).

[37] R. Sari, T. Piran, and R. Narayan, Astrophys. J. **497**, L17 (1998).

[38] J. Granot, A. Panaitescu, P. Kumar, and S. E. Woosley, Astrophys. J. **570**, L61 (2002).

[39] E. M. Rossi, D. Lazzati, J. D. Salmonson, and G. Ghisellini, Mon. Not. R. Astron. Soc. **354**, 86 (2004).

[40] E. Nakar and R. Sari, Astrophys. J. **747**, 88 (2012).

[41] A. Panaitescu and P. Kumar, Astrophys. J. **543**, 66 (2000).

[42] A. Panaitescu and P. Mészáros, Astrophys. J. **493**, L31 (1998).

[43] J. E. Rhoads, Astrophys. J. **487**, L1 (1997).

[44] H. van Eerten, W. Zhang, and A. MacFadyen, Astrophys. J. **722**, 235 (2010).

[45] W. Fong, E. Berger, R. Margutti, and B. A. Zauderer, Astrophys. J. **815**, 102 (2015).

[46] A. Murguia-Berthier, G. Montes, E. Ramirez-Ruiz, F. De Colle, and W. H. Lee, Astrophys. J. **788**, L8 (2014).

[47] H. Nagakura, K. Hotokezaka, Y. Sekiguchi, M. Shibata, and K. Ioka, Astrophys. J. **784**, L28 (2014).

[48] P. C. Duffell, E. Quataert, and A. I. MacFadyen, Astrophys. J. **813**, 64 (2015).

[49] A. Murguia-Berthier, E. Ramirez-Ruiz, G. Montes, F. De Colle, L. Rezzolla, S. Rosswog, K. Takami, A. Perego, and W. H. Lee, Astrophys. J. **835**, L34 (2017).

[50] H. J. van Eerten and A. I. MacFadyen, Astrophys. J. **733**, L37 (2011).

[51] J. Granot, D. Guetta, and R. Gill, Astrophys. J. **850**, L24 (2017).

[52] J. Granot, R. Gill, D. Guetta, and F. De Colle, arXiv:1710.06421 [Mon. Not. R. Astron. Soc. (to be published)].

[53] G. P. Lamb and S. Kobayashi, arXiv:1710.05857 [Mon. Not. R. Astron. Soc. (to be published)].

[54] Y.-C. Zou, F.-F. Wang, R. Moharana, B. Liao, W. Chen, Q. Wu, W.-H. Lei, and F.-Y. Wang, Astrophys. J. **852**, L1 (2018).

[55] L. Resmi, S. Schulze, C. H. I. Chandra, K. Misra, J. Buchner, M. De Pasquale, R. S. Ramirez, S. Klose, S. Kim, N. R. Tanvir, and P. T. O'Brien, arXiv:1803.02768 [Astrophys. J. (to be published)].

[56] D. Dobie, D. L. Kaplan, T. Murphy, E. Lenc, K. P. Mooley, C. Lynch, A. Corsi, D. Frail, M. Kasliwal, and G. Hallinan, arXiv:1803.06853.

[57] J. D. Lyman *et al.*, arXiv:1801.02669.

[58] E. Troja, L. Piro, G. Ryan, H. van Eerten, R. Ricci, M. Wieringa, S. Lotti, T. Sakamoto, and S. B. Cenko, arXiv:1801.06516 [Mon. Not. R. Astron. Soc. (to be published)].

[59] K. D. Alexander, R. Margutti, P. K. Blanchard, W. Fong, E. Berger, A. Hajela, T. Eftekhari, R. Chornock, P. S. Cowperthwaite, D. Giannios, C. Guidorzi, A. Kathirgamaraju, A. MacFadyen, B. D. Metzger, M. Nicholl, L. Sironi, V. A. Villar, P. K. G. Williams, X. Xie, and J. Zrake, arXiv:1805.02870.

[60] G. Ghirlanda, O. S. Salafia, A. Pescalli, G. Ghisellini, R. Salvaterra, E. Chassande-Mottin, M. Colpi, F. Nappo, P. D'Avanzo, A. Melandri, M. G. Bernardini, M. Branchesi, S. Campana, R. Ciolfi, S. Covino, D. Götz, S. D. Vergani, M. Zennaro, and G. Tagliaferri, Astron. Astrophys. **594**, A84 (2016).

[61] E. Nakar, Phys. Rep. **442**, 166 (2007).

[62] D. Eichler, M. Livio, T. Piran, and D. N. Schramm, Nature (London) **340**, 126 (1989).

[63] E. Berger, Annu. Rev. Astron. Astrophys. **52**, 43 (2014).

[64] A. Perego, D. Radice, and S. Bernuzzi, Astrophys. J. **850**, L37 (2017).

[65] R. Gill and J. Granot, arXiv:1803.05892 [Mon. Not. R. Astron. Soc. (to be published)].

[66] E. Nakar, O. Gottlieb, T. Piran, M. M. Kasliwal, and G. Hallinan, arXiv:1803.07595.